Journal of Sound and Vibration (1997) **206**(2), 133–149

THE USE OF MAGNETOSTRICTIVE PARTICLE ACTUATORS FOR VIBRATION ATTENUATION OF FLEXIBLE BEAMS

A. V. Krishna Murty

Department of Aerospace Engineering, Indian Institute of Science, Bangalore 560 012, *India*

and

M. Anjanappa and Y.-F. Wu

Department of Mechanical Engineering, University of Maryland—UMBC, Baltimore, Maryland 21228, *U.S.A.*

(*Received* 29 *March* 1996, *and in final form* 17 *February* 1997)

A laminated composite beam, representative of a flexible beam, containing a layer of magnetostrictive material, is considered as a distributed parameter system and its dynamic behavior has been investigated. The magnetostrictive layer is used to induce actuation forces to control vibration in the beam, following a velocity feedback control law. The dynamic behavior of the beam is studied to illustrate the effect of the lay-up sequence, the weight of the coil, the control gain and the concentrated mass on the vibration suppression capability. Numerical results have been given for three different lay-up sequences of the laminates, representing a wide range of stiffness variation. The controllability of the first four modes, the corresponding coil current and the stresses have also been discussed. The results clearly indicate viability of developing a smart flexible beam with embedded magnetostrictive particle layers.

1. INTRODUCTION

Flexible robot manipulators are used in many modern industries, such as the automobile, electronic and aerospace industries, to achieve high speed automation. They are usually in the form of cantilever beams attached to a rotor, intended to pick up a payload at a source point and deliver it smoothly at its destination in a horizontal plane. This study is restricted to horizontal plane motion, as it represents the most common motion encountered in the pick and place type of robot. At the time of delivering the object, a certain amount of vibration of the beam is unavoidable, as it is highly flexible. The reduction of such vibration improves the performance of the robot. Although passive damping reduces vibration, it is now well recognized that to achieve significant improvement in the overall performance of flexible robot manipulators, new technologies should be explored. Smart robots using smart structures technology are one promising candidate. They typically have integrated sensors and actuators interconnected by adaptive real time controllers. Among others, the most promising candidate materials for sensors and actuators are shape memory alloys, piezoelectric and magnetostrictive materials. Vibration suppression of flexible beams using shape memory alloy and piezoelectric actuators have received considerable attention (see, for example, references [1–3]).

0022–460X/97/370133 + 17 $25.00/0/sv970997

However, there appear to be no investigation, so far, on the use of magnetostrictive materials for flexible beam application. The purpose of this paper is to bring out the effectiveness of the magnetostrictive materials for this application.

The magnetostrictive material, Terfenol-D, has certain unique advantages over other materials, such as (1) the possibility of remote excitation (2) the ability to retain the magnetostrictive property both in a bulk form such as rods and in a particle form, and (3) easy embedability into the host material. In particular, the magnetostrictive material in particle form can be embedded into modern fiber reinforced plastic layered composites without compromising the structural integrity. Notwithstanding the disadvantage of the higher density of this material as compared to other smart materials, it can still be viewed as an attractive candidate for developing vibration control technology for certain applications, such as robot manipulators, in view of the feasibility of realizing higher actuation forces and the consequent gains in performance.

Broadly, the vibration control of smart structures can be attempted in two ways; viz., discrete actuation and distributed actuation. As early as 1957, Wise [4] reported the feasibility of using the magnetostrictive property to develop actuation forces. Magnetostriction-based discrete actuation has attracted research interest ever since (see, for example references 5–7]). In reference [8], the usefulness of magnetostrictive material for helicopter rotor servoflap control has been demonstrated. Recently, the development of compact magnetostrictive mini-actuators for smart structure applications has been reported by the authors [9, 10]. Magnetostrictive material, under the name of Terfenol-D, is now available both in bulk as well as particle form. Most of the investigations to date propose the use of this material in bulk form. However, smart structure technology based on the particle form is more attractive from the standpoint of manufacturing, since the magnetostrictive material in particle form can be easily embedded in laminated composites. In the present study, we use this approach.

The magnetostrictive particle layer exhibits the same constitutive relationship as the monolithic layer. However, the magnetomechanical coupling coefficient differs, being dependent on the prestress, the magnetic field and the orientation. For purposes of illustration, in this work, we have assumed perfect orientation and zero pre-stress. Hence, when a magnetic field is applied, the magnetostrictive particle layers elongate, following the same constitutive equations as the monolithic layer.

A flexible cantilever laminated composite beam containing an embedded layer of Terfenol-D particles has been investigated. Choosing a velocity feedback constant gain control, the feasibility of vibration reduction is demonstrated.

2. FORMULATION

A typical composite beam representative of a flexible beam is shown in Figure 1. It is considered as a cantilever beam fixed to the rotor at $x = 0$ and free at $x = L$, carrying a payload of mass m_0 at a distance L_3 from the fixed end. The beam is made up of n layers with n-l layers of CFRP (Carbon Fiber Reinforced Plastic) plies and one layer of Terfenol-D particles. The Terfenol-D particles in the mth layer, located at a distance $\bar{y}$, are set in a suitable resin, such as epoxy, and bonded to the neighboring CFRP layers without any possibility of slip. In the present analysis the weight of the resin in the mth layer is ignored. A series of closely packed magnetic coils, insulated from each other, enclose the beam over a part of the beam from L_1 to L_2. By applying the required current to these coils, the necessary magnetic field intensity and hence the actuation stress are induced in the Terfenol-D layer in the region L_1 to L_2. The widths of the coils are made

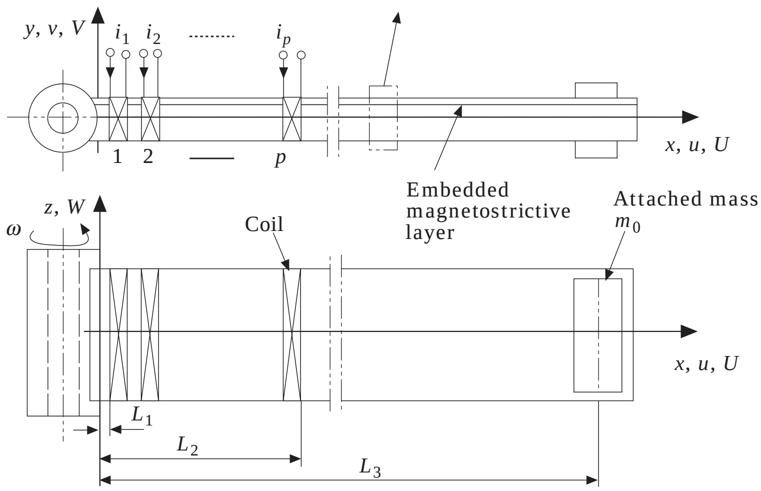

(a)

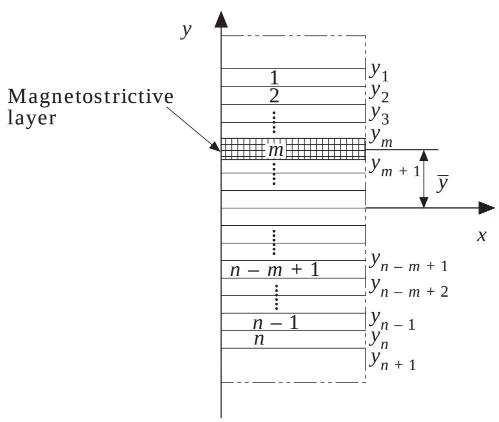

(b)

Figure 1. A typical laminate composite beam (a) with an embedded magnetostrictive layer (b).

as small as possible to enable a required variation of control forces in this region. All CFRP layers are assumed to behave as a linear orthotropic medium, whereas the Terfenol-D layer behaves as an equivalent isotropic medium. The fiber orientations in CFRP layers are arbitrary. The cross-section of the beam is assumed to be uniform about the z-axis. The deformations in the x–z plane are infinitesimally small, since the beam has very high flexural stiffness in the x–z plane as compared to the x–y plane. At first the beam has no applied dynamic forces.

At the instant at which the rotor stops, when the destination is reached, it is assumed that the beam receives an applied velocity profile according to the mode shape of the beam. This velocity is considered as initial velocity with a zero initial displacement. The dynamic motion of the beam subsequent to this instant may be modelled by considering the displacement field in the form,

$$U(x, y, z, t) = u(x, t) - yv_{,x}, \qquad V(x, y, z, t) = v(x, t), \qquad W(x, y, z, t) = 0. \tag{1}$$

The term u in the expression U is included to take into consideration the extension effect arising due to asymmetry in the lay-up of the beam.

The strain field consists of a single non-zero component of strain,

$$\epsilon_x = u_{,x} - y v_{,xx}. \tag{2}$$

The constitutive relation of all CFRP layers [11] is of the form

$$\sigma_x^{(i)} = \bar{Q}_{11}^{(i)} \varepsilon_x^{(i)}, \tag{3}$$

where the superscript i represents the layer number and

$$\begin{gathered} \bar{Q}_{11}^{(i)} = Q_{11}^{(i)} \cos^4 \theta^{(i)} + 2(Q_{12}^{(i)} + 2Q_{66}^{(i)}) \cos^2 \theta^{(i)} \sin^2 \theta^{(i)} + Q_{22}^{(i)} \sin^4 \theta^{(i)}, \\ Q_{11}^{(i)} = E_{11}^{(i)}/(1 - \nu_{12}^{(i)} \nu_{21}^{(i)}), \qquad Q_{22}^{(i)} = E_{22}^{(i)}/(1 - \nu_{12}^{(i)} \nu_{21}^{(i)}), \\ Q_{12}^{(i)} = Q_{21}^{(i)} = \nu_{21}^{(i)} E_{11}^{(i)}/(1 - \nu_{12}^{(i)} \nu_{21}^{(i)}), \qquad Q_{66}^{(i)} = G_{12}^{(i)}. \end{gathered} \tag{4}$$

The constitutive relation of the magnetostrictive layer is [12],

$$\varepsilon_x = S\sigma + dH, \tag{5}$$

Considering the closed loop velocity proportional feedback control, the magnetic field intensity is expressed as,

$$H(x, t) = k_1 I(x, t) \qquad \text{for } L_1 \leqslant x \leqslant L_2, \tag{6}$$

where $I(x, t) = g(t)\dot{v}(x, t)$, k_1 is the coil constant, and g is the control gain. Rewriting equation (6), we obtain $H(x, t) = c\dot{v}(x, t)$, where $c = k_1 g$.

Since it is difficult to obtain the exact solution for a cantilever beam, we attempt an approximate solution, starting with

$$v(x, t) = \sum_{k=1}^{n} \Lambda_1^{(k)}(t) X_1^{(k)}(x), \qquad u(x, t) = \sum_{k=1}^{n} \Lambda_2^{(k)}(t) X_2^{(k)}(x), \tag{7}$$

where $0 \leqslant x \leqslant L$, $t \geqslant 0$. Λ_1 and Λ_2 are functions of t to be determined, X_1 and X_2 are functions of x to be chosen, and superscript k refers to the mode number. In the interests of simplicity, in the present analysis it is assumed that the eigenfunctions of the beam are uncoupled, as

$$\begin{gathered} X_1^{(k)} = a_k\left(\sin \frac{C_k}{L} x - \sinh \frac{C_k}{L} x\right) + b_k\left(\cos \frac{C_k}{L} x - \cosh \frac{C_k}{L} x\right), \\ X_2^{(k)} = \sin \frac{(2k-1)\pi x}{2L}, \qquad k = 1, 2, \ldots, \end{gathered} \tag{8}$$

where $a_k = \sin C_k - \sinh C_k$ and $b_k = \cos C_k + \cosh C_k$. In the first part of equation (8), the eigenfunctions correspond to the transverse vibration of a cantilever beam. The eigenfunction in the second part of equation (8) represents the eigenfunction of a longitudinal vibration of a uniform thin beam.

For the first four modes, the value of C_k are given as, $C_1 = 1{\cdot}875$, $C_2 = 4{\cdot}694$, $C_3 = 7{\cdot}855$, and $C_4 = 11{\cdot}0$. For example, $k = 1$ corresponds to the response considering only the first mode, which is the largest in most cases. In the present study we are interested in the response due to application of an initial velocity profile distribution of the type,

$$\dot{v}^{(k)}(x, 0) = \sum_{k=1}^{n} X_1^{(k)}(x) \dot{\Lambda}_1^{(k)}(0), \tag{9}$$

with $\dot{\Lambda}_1^{(k)}(0) = 1$ for $k = 1, 2, 3, 4$. The responses of higher modes are also estimated in a qualitative sense by the present procedure, as it ignores the coupling between modes arising out of feedback control and does not include the effect of spillover. However, the main coupling effect between longitudinal and transverse motion is retained. Hence, in what follows, the formulation is applicable for each mode and the superscript k is dropped for convenience.

Consider the Hamilton's principle in the form,

$$\delta \int_{t_1}^{t_2} (U_e - T_e)\,\mathrm{d}t \equiv 0, \tag{10}$$

where

$$U_e = \tfrac{1}{2}\int_\Omega \sigma_x \varepsilon_x \,\mathrm{d}\Omega, \qquad T_e = \tfrac{1}{2}\int_\Omega \rho(\dot{u}^2 + \dot{v}^2)\,\mathrm{d}\Omega, \tag{11}$$

and where $\Omega \subset R^3$; that is, the volume of the beam. In the above equation, ε_x includes the strain due to the magnetostrictive actuation, as given by equation (5).

Using this form of Hamilton's principle, the governing equations of motion are deduced as,

$$(A\Lambda_2 + M_2\ddot{\Lambda}_2) - (B\Lambda_1 + F_1 c\dot{\Lambda}_1) = 0, \qquad (-B\Lambda_2 + F_2 c\dot{\Lambda}_2) + (D\Lambda_1 + M_1\ddot{\Lambda}_1) = 0, \tag{12}$$

where

$$A = \int_x \int_y \bar{Q}_{11}^{(i)} X_{2,x}^2 \,\mathrm{d}x\,\mathrm{d}y = \int_0^L X_{2,x}^2\,\mathrm{d}x \sum_{i=j}^{n} \bar{Q}_{11}^{(i)}(y_{i+1} - y_i),$$

$$B = \int_x \int_y \bar{Q}_{11}^{(i)} X_{1,xx} X_{2,x}\, y \,\mathrm{d}x\,\mathrm{d}y = \int_0^L X_{1,xx}X_{2,x}\,\mathrm{d}x \sum_{i=1}^{n} \bar{Q}_{11}^{(i)}\left(\frac{y_{i+1}^2 - y_i^2}{2}\right), \tag{13}$$

$$D = \int_x \int_y \bar{Q}_{11}^{(i)} X_{1,xx}^2 y^2 \,\mathrm{d}x\,\mathrm{d}y = \int_0^L X_{1,xx}^2\,\mathrm{d}x \sum_{i=1}^{n} \bar{Q}_{11}^{(i)}\left(\frac{y_{i+1}^3 - y_i^3}{3}\right),$$

$$F_1 = \int_x \int_y \bar{Q}_{11}^{(i)} X_{1,x} X_{2,x}\, d \,\mathrm{d}x\,\mathrm{d}y = dE_m(y_{m+1} - y_m)\int_{L_1}^{L_2} X_{1,x}X_{2,x}\,\mathrm{d}x,$$

$$F_2 = \int_x \int_y \bar{Q}_{11}^{(i)} X_{1,x} X_{1,xx}\, y d \,\mathrm{d}x\,\mathrm{d}y = dE_m\left(\frac{y_{m+1}^2 - y_m^2}{2}\right)\int_{L_1}^{L_2} X_{1,x}X_{1,xx}\,\mathrm{d}x,$$

$$M_1 = \int_0^L mX_1^2\,\mathrm{d}x + \int_{L_1}^{L_2} m_c X_1^2\,\mathrm{d}x + m_0 X_1^2(L_3),$$

$$M_2 = \int_0^L mX_2^2\,\mathrm{d}x + \int_{L_1}^{L_2} m_c X_2^2\,\mathrm{d}x + m_0 X_2^2(L_3).$$

The detailed boundary value problem is given in Appendix A. Considering the form $(\Lambda_1, \Lambda_2) = (Y_1, Y_2)\,\mathrm{e}^{\lambda t}$ and substituting in equations (12) for the non-trivial solution, we obtain,

$$\begin{vmatrix} A + M_2\lambda^2 & -(B + F_1 c\lambda) \\ -B & D + F_2 c\lambda + M_1\lambda^2 \end{vmatrix} \equiv 0. \tag{14}$$

Equation (14) gives two sets of complex eigenvalues, one representing primarily transverse motion and the other primarily axial motion. Frequencies associated with the axial motion are very high in slender flexible beams as compared to frequencies associated with transverse motion. Since we are concerned with primarily transverse motion, the eigenvalue of interest is the lower one of the form

$$\lambda = -\alpha \pm \mathrm{j}\omega_d. \tag{15}$$

Consider initial conditions of the type,

$$\Lambda_1 = \Lambda_2 = \dot{\Lambda}_2 = 0, \qquad \dot{\Lambda}_1 = 1. \tag{16}$$

The expressions for u and v may be obtained as

$$v = \frac{X_1(x)}{\omega_d}\,\mathrm{e}^{-\alpha t} \sin \omega_d t, \qquad u = \frac{X_2(x)}{\omega_d}\,\phi\,\mathrm{e}^{-\alpha t} \sin \omega_d t, \tag{17}$$

where

$$\phi = \frac{-(B + F_1 c\lambda)}{A + M_2\lambda^2}, \tag{18}$$

In other words, ϕ is the ratio of the magnitude of generalized time coordinate of longitudinal vibration over the magnitude of generalized time coordinate of transverse vibration.

From equation (5) it follows that the actuation stress in the magnetostrictive layer for velocity proportional feedback control is

$$\sigma_a(x, t) = -E_m d H(x, t), \tag{19}$$

where

$$H(x, t) = c\dot{v}(x, t) \qquad \text{for } L_1 \leqslant x \leqslant L_2. \tag{20}$$

Now, from equations (17) and (19), the actuation stress can be obtained as,

$$\sigma_a(x, t) = -\frac{E_m d c X_1(x)}{\omega_d} \frac{\mathrm{d}}{\mathrm{d}t}\left[\mathrm{e}^{-\alpha t} \sin(\omega_d t)\right] \qquad \text{for } L_1 \leqslant x \leqslant L_2. \tag{21}$$

2.1. CURRENT REQUIREMENT

From equations (6), it follows that the general expression for the coil current is,

$$I(x, t) = (c/k_1)\dot{v}(x, t), \tag{22}$$

based on the standard circular coil [13], where the magnetic field at the center is given as $H = (NI)/\sqrt{l^2 + 4r_c^2} = k_1 I$. We can obtain the constant k_1 by assuming that the region between L_1 and L_2 is divided into p coils with an equivalent radius r_c as (see Figure 1)

$$k_1 = n_0 \left(1 + \frac{4r_c^2 p^2}{(L_2 - L_1)^2}\right)^{-1/2}, \tag{23}$$

where, n_0 is the number of turns per unit length of the coil.

The current in the qth coil can be written as,

$$I(x_q, t) = (c/k_1) X_1(x_q) \dot{A}_1(t), \tag{24}$$

where

$$x_q = L_1 + (2q - 1)(L_2 - L_1)/(2p) \qquad \text{for } q = 1, 2, \ldots, p. \tag{25}$$

$I(x_q, t)$ can be written in another form:

$$I(x_q, t) = \frac{c}{k_1 \omega_d} X_1(x_q) \frac{\mathrm{d}}{\mathrm{d}t} [\mathrm{e}^{-\alpha t} \sin(\omega_d t)]. \tag{26}$$

3. NUMERICAL RESULTS AND DISCUSSION

The lay-up sequences of three laminated beams studied are shown in Table 1. Here m represents the magnetostrictive layer and other numbers represent the fiber angles with respect to the *x-axis* in the x–z plane in the CFRP layers. For example in $[\pm 45/0_2/90_2/0/\pm 45/\mathrm{m}]$, "$\pm 45$" denotes one layer with a fiber angle of $+45$ degrees and the next layer with fiber angle of -45 degrees. The "/" is used to separate the adjacent layers with different fiber angles. The next layers are denoted by "0_2", where the subscript "2" denotes the number of layers with the same fiber angle, so two layers with a fiber angle of 0 degrees are used. "m" is an abbreviation for "magnetostrictive particle layer". All beams considered have ten layers of 1 mm thickness each. The material properties of the CFRP layers are $E_{11} = 138{\cdot}6$ GPa, $E_{22} = 8{\cdot}27$ GPa, $G_{12} = 4{\cdot}14$ GPa, $v_{12} = 0{\cdot}26$ and $\rho = 1824$ kg/m^3. The properties of the Terfenol-D layer are $E_\mathrm{m} = 26{\cdot}5$ GPa, $\rho_m = 9250$ kg/m^3 and $d = 1{\cdot}67 \times 10^{-8}$ m/A. The effective radius of coils enclosing the magnetostrictive layer r_c is taken to be 10 mm, with the coil density, n_o turns/meter, made up of 38 AWG copper wires with a density of 8844 kg/m^3. For all numerical investigations, $L = 1$ m and $L_1 = 0$. The range 0–L_2 is divided into ten coils, and are numbered from 1 to 10 starting from the fixed end (see Figure 1). Ten coils were chosen for illustration purposes and the number have no other significance. The weight of coil per unit length with $n_0 = 10^4$ is 3·15 kg, whereas it is 31·54 kg with $n_0 = 10^5$.

In Figures 2–5 are shown the results of first four modes separately for the case $L_2 = 0{\cdot}6$ m, $L_3 = 0{\cdot}9$ m, $m_0 = 1$ kg, and $c = 10^4$. A comparison of the uncontrolled and controlled transverse motion of the tip of the cantilever beam is shown in Figures 2a–5a.

TABLE 1

Details of the laminates studied

Laminate number	Lay-up sequence
1	$[\pm 45/0_2/90_2/0/\pm 45/\mathrm{m}]$
2	$[90_9/\mathrm{m}]$
3	$[0_9/\mathrm{m}]$

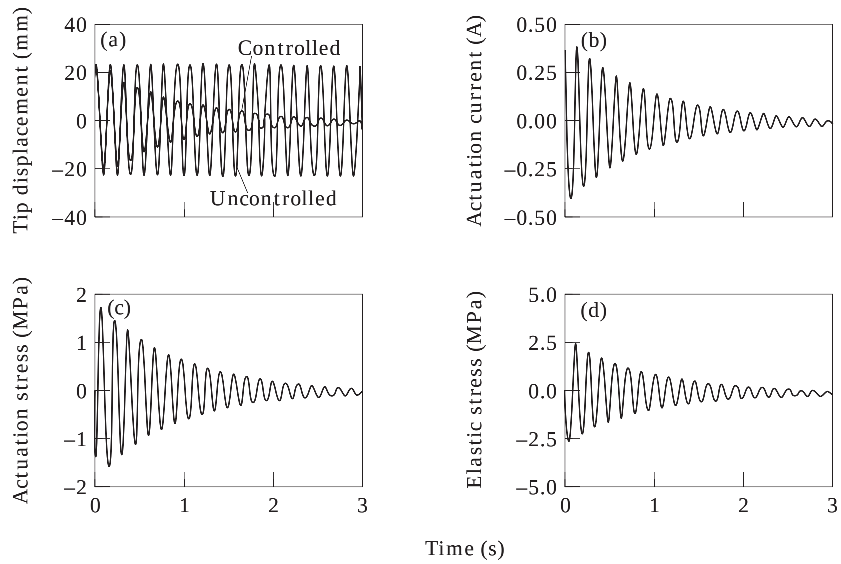

Figure 2. Vibration suppression: the fundamental mode ($\omega_1 = 43{\cdot}43$ rad/s, $\alpha_1 = -1{\cdot}09$ rad/s). (a) Variation of the tip displacement; (b) the control current in the tenth coil; (c) the actuation stress at $0{\cdot}57L$; (d) the elastic stress at $0{\cdot}57L$.

It may be noted that the fundamental mode is suppressed in about 4 seconds, whereas the second, third and fourth modes are suppressed in about 1·5, 0·5 and 0·2 s, respectively. Similarly, the variation of current in the coil carrying the highest current is shown in Figures 2(b)–5(b). It may also be noted that different coils require different levels of current to generate a coordinated vibration suppression action. In the present analysis, the coil

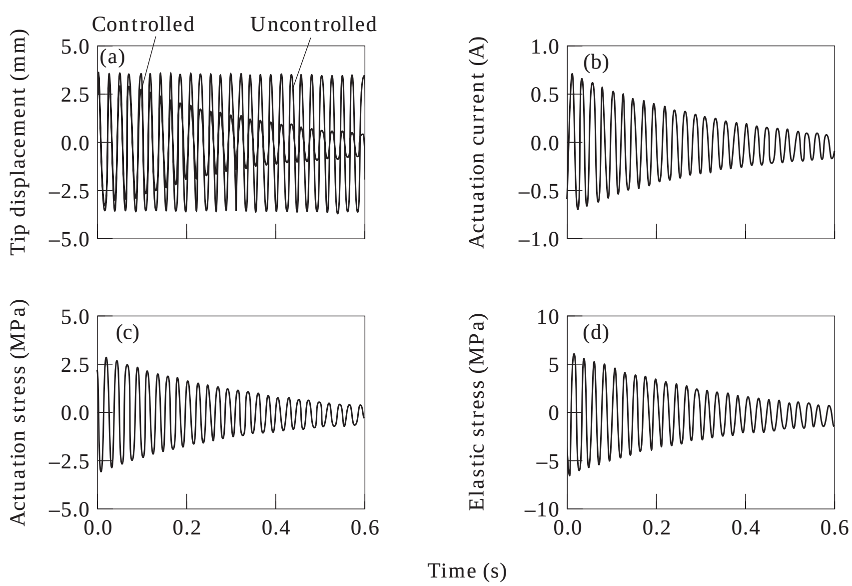

Figure 3. Vibration suppression: the second mode ($\omega_2 = 266{\cdot}84$ rad/s, $\alpha_2 = -2{\cdot}77$ rad/s). (a) Variation of the tip displacement; (b) the control current in the eight coil; (c) the actuation stress at $0{\cdot}45L$; (d) the elastic stress at $0{\cdot}45L$.

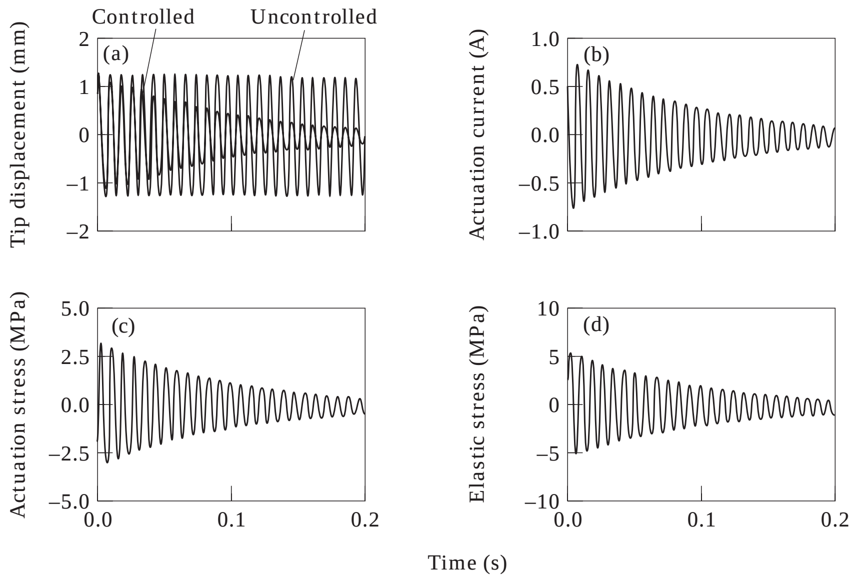

Figure 4. Vibration suppression: the third mode ($\omega_3 = 762{\cdot}14$ rad/s, $\alpha_3 = -9{\cdot}17$ rad/s). (a) variation of the tip displacement; (b) the control current in the fifth coil; (c) the actuation stress at $0{\cdot}27L$; (d) the elastic stress at $0{\cdot}27L$.

currents are proportional to the velocity at the location of the coil. Hence, different coils are selected as the primary coil to suppress the vibration in different modes as illustrated in these figures. It may be noted that the maximum current required varies from mode to mode, from about 400 mA to 800 mA. The actuation stresses induced by the coil

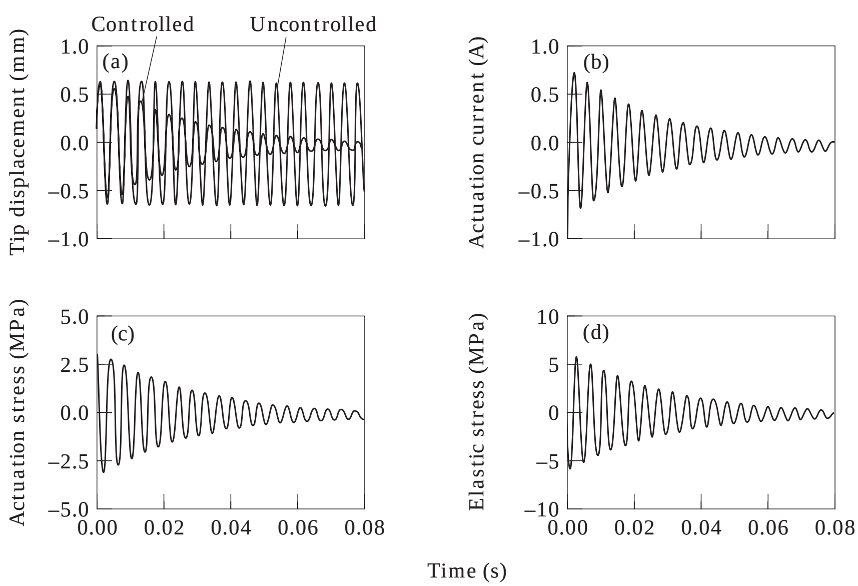

Figure 5. Vibration suppression: the fourth mode ($\omega_4 = 1490{\cdot}08$ rad/s, $\alpha_4 = -32{\cdot}46$ rad/s). (a) Variation of the tip displacement; (b) the control current in the fourth coil; (c) the actuation stress at $0{\cdot}21L$; (d) the elastic stress at $0{\cdot}21L$.

carrying the maximum current are given in Figures 2(c)–5(c). The elastic stresses in the magnetostrictive layer are shown in Figures 2d–5d for various modes. Both the elastic and actuation stresses are in the range 3–5 MPa, well within the allowable stress for magnetostrictive materials.

To illustrate the effect of coupling between longitudinal motion (along the x-axis) and the vibration characteristics of the beam, two cases are studied. The results obtained are shown in Table 2. Case 1 refers to the results obtained when the longitudinal inertia due to M_2 is included, whereas case 2 represents the results when the coupling is neglected. Inspection of Table 2 shows that the effect of M_2 has a negligible influence on ω_d and ϕ. The ratio of longitudinal to transverse motion, ϕ is less than one percent in all three laminates considered. However, the coupling has some influence on ω_d and α. The influence on α is of the order of 5–6% and that on ω_d is less than 1%. The parameter α plays a significant role in the present study, as it represents the damping pattern. Hence, this coupling is included in all calculations.

Laminate 1 was chosen to study the influence of coil mass. The results are tabulated in Table 3. By neglecting coil mass ω_d becomes overestimated slightly, by about 0·5% at the fourth mode. The influence on α is much larger, of the order of 8–9%, and it has little influence on ϕ. It may be noted that the coil mass is about 9·5% of the beam mass distributed in a region of about 60% of the span near the cantilever fixed end, and so the relatively small effects on ω_d and ϕ are to be expected. However, since its influence on α is significant, the coil mass cannot be ignored.

Next, the effect of coil span length is explored. From Figure 1, it may be noted that the coils enclosing the magnetostrictive layer cover only part of the span of the beam and the total range of the ten *coils* put together is L_2. Results for three values of L_2 are given in Table 4. t_s is the vibration suppression time. For purpose of this work, $\pm 2\%$ error is chosen as the acceptable error. Reduction of L_2 has very little effect on ω_d as should be expected. However, the values of α are substantially affected resulting in large influence on vibration suppression times. For example, the vibration suppression time for the first mode is 4 s when $L_2 = 0{\cdot}6$ m, whereas the time increases to 15 s when L_2 is reduced to 0·2 m. However, it may be noted that in the case of higher modes, this is not always true. For example, the second mode becomes suppressed faster with $L_2 = 0{\cdot}2$ m than with $L_2 = 0{\cdot}4$ m. This variation suggests that for each mode, the best location of the coil is different perhaps coinciding with highly stressed areas of the beams. This needs further detailed investigation.

The effect of increasing the weight of the concentrated mass located at $0{\cdot}7L$ from 1 kg to 3 kg is shown in Table 5. The frequencies reduce by a small amount as expected. The absolute value of α also decreases from 5%–10%. The corresponding plots obtained for the first mode are shown in Figures 6 and 7. No significant loss of vibration suppression time due to an increase in the weight of the concentrated mass can be observed.

In Table 6, two cases with an order of magnitude increase in control gain parameter and number of turns in the coil are compared. Case 1, with $c = 10^4$, has twice the coil span length compared to that of Case 2, whose control gain of which is $c = 10^5$. The vibration suppression times T and the highest initial coil current I are also given. This data indicates that even with a small coil span of $0{\cdot}1L$, it is possible to control the first four modes. It may be noted that the coil current with $c = 10^5$ is somewhat high for higher modes, which of course can be brought down by a further increase of coil turns.

Finally, the effect of flexural rigidity on the vibration suppression is studied. Amongst the ten layered beams considered here, $[90_9/\mathrm{m}]$ has the lowest flexural rigidity

TABLE 2

The influence of coupling with longitudinal motion

Mode number	ω_n	Case 1 ω_d	Case 1 α	Case 1 ϕ	Case 2 ($u = 0$) ω_d	Case 2 ($u = 0$) α	Case 2 ($u = 0$) ϕ	Other parameters of the beam
1	42·429	42·416	−1·085	0·00007	42·475	−1·095	0	Laminate 1;
2	266·843	266·83	−2·769	0·00039	267·612	−2·828	0	$L_2 = 0{\cdot}6$ m, $L_3 = 0{\cdot}9$ m,
3	762·136	762·081	−9·166	0·00093	764·618	−10·379	0	$m_c = 3{\cdot}15$ kg/m, $m_0 = 1$ kg,
4	1490·08	1489·73	−32·464	0·00136	1494·99	−33·886	0	$c = 10^4$, $n_0 = 10^4$ turns/m
1	43·924	43·917	−0·086	0·00008	43·979	−0·789	0	Laminate 2;
2	279·923	279·033	−22·31	0·00058	279·921	−21·479	0	$L_2 = 0{\cdot}1$ m, $L_3 = 0{\cdot}7$ m,
3	762·553	754·935	−107·52	0·0019	758·205	−102·53	0	$m_c = 31{\cdot}5$ kg/m, $m_0 = 1$ kg,
4	1518·71	1495·98	−244·76	0·0039	1503·70	−230·47	0	$c = 10^5$, $n_0 = 10^5$ turns/m
1	62·023	62·019	−0·728	0·00006	62·071	−0·715	0	Laminate 3;
2	409·165	408·601	−21·480	0·00043	409·339	−20·837	0	$L_2 = 0{\cdot}1$ m, $L_3 = 0{\cdot}7$ m,
3	1066·88	1062·68	−94·628	0·00136	1065·09	−91·094	0	$m_c = 31{\cdot}5$ kg/m, $m_0 = 3$ kg,
4	2198·45	2186·30	−230·86	0·00281	2192·02	−219·99	0	$c = 10^5$, $n_0 = 10^5$ turns/m

TABLE 3

The effect of coil mass

Mode number	Coil mass neglected ($m_c = 0$) ω_d	Coil mass neglected ($m_c = 0$) α	Coil mass neglected ($m_c = 0$) ϕ	Coil mass included ($m_c = 3{\cdot}15$ kg/m) ω_d	Coil mass included ($m_c = 3{\cdot}15$ kg/m) α	Coil mass included ($m_c = 3{\cdot}15$ kg/m) ϕ	Other beam parameters
1	42·682	−1·099	0·00007	42·415	−1·085	0·00007	Laminate 1;
2	276·371	−2·971	0·00039	266·829	−2·769	0·00039	$L_2 = 0{\cdot}6$ m, $L_3 = 0{\cdot}9$ m,
3	786·673	−9·770	0·00093	762·081	−9·166	0·00092	$n_0 = 10^4$ turns/m,
4	1546·940	−35·007	0·00136	1489·729	−32·464	0·00136	$m_0 = 1$ kg, $c = 10^4$

TABLE 4

The effect of span length over which the coil encloses the magnetostrictive layer (*laminate* 1, $L_3 = 0{\cdot}9L$, $n_0 = 10^4$ turns/m, $m_c = 3{\cdot}15$ kg, $m_0 = 1$ kg, $c = 10^4$)

Mode number	$L_2 = 0{\cdot}6$ m			$L_2 = 0{\cdot}4$ m			$L_2 = 0{\cdot}2$ m		
	ω_d	α	t_s	ω_d	α	t_s	ω_d	α	t_s
1	42·415	−1·085	4	42·648	−0·732	5	42·695	−0·261	15
2	266·829	−2·769	1·5	272·576	−0·673	5	276·081	−4·167	1
3	762·081	−9·166	0·5	765·233	−12·514	0·3	782·855	−7·866	0·5
4	1489·73	−32·46	0·2	1513·348	−37·444	0·1	1531·53	−0·918	5

and the $[0_9/m]$ laminate has the highest flexural rigidity, and the performance of these beams is compared in Table 7. Low values of ϕ in these two extreme cases justify the neglect of longitudinal inertia for this class of beams. The value of α indicates that it is possible to suppress the vibration in a reasonable time. The details of the vibration suppression of the fundamental mode are shown in Figures 8 and 9. The pattern is the same for higher modes as well.

In the present analysis, all coils receive current as per the control law, which has a constant gain for the entire span. Results indicate that higher modes do not always become suppressed with an equal facility as the fundamental mode, although, generally, higher modes also become suppressed. It may be expedient to provide different gains to different coils to achieve the required pattern of vibration suppression. Furthermore, the choice of velocity proportional feedback was driven by the desire to keep the mathematics simple and emphasize the feasibility. A control law that uses a relative angular velocity as the feedback signal would be more efficient. It is also possible to use some of the coils for sensing and the rest for actuation, to develop an integrated smart structural system. These aspects deserve further investigation.

4. CONCLUSIONS

A cantilevered laminated composite beam, representative of a flexible robot manipulator, containing a layer of magnetostrictive particles has been investigated to bring out the vibration suppression possibilities. Ten closely spaced coils spread over part of the beam from the fixed end are used to induce actuation stresses in the magnetostrictive layer. Keeping in view possible application to robot arms, a concentrated mass located at a certain distance on the span is also included. The system is modelled as a distributed parameter system. The response of the beam in the first four modes to

TABLE 5

The effect of concentrated mass m_0 (*laminate* 1, $c = 10^5$, $L_2 = 0{\cdot}1L$, $n_0 = 10^5$ turns/m, $m_c = 31{\cdot}5$ kg/m)

Mode number	$L_3 = 0{\cdot}7$ m, $m_0 = 1$ kg		$L_3 = 0{\cdot}7$ m, $m_0 = 3$ kg	
	ω_d	α	ω_d	α
1	43·916	−0·806	41·813	−0·731
2	279·033	−22·311	274·855	−21·643
3	754·935	−107·521	712·392	−95·527
4	1495·984	−244·758	1462·454	−233·624

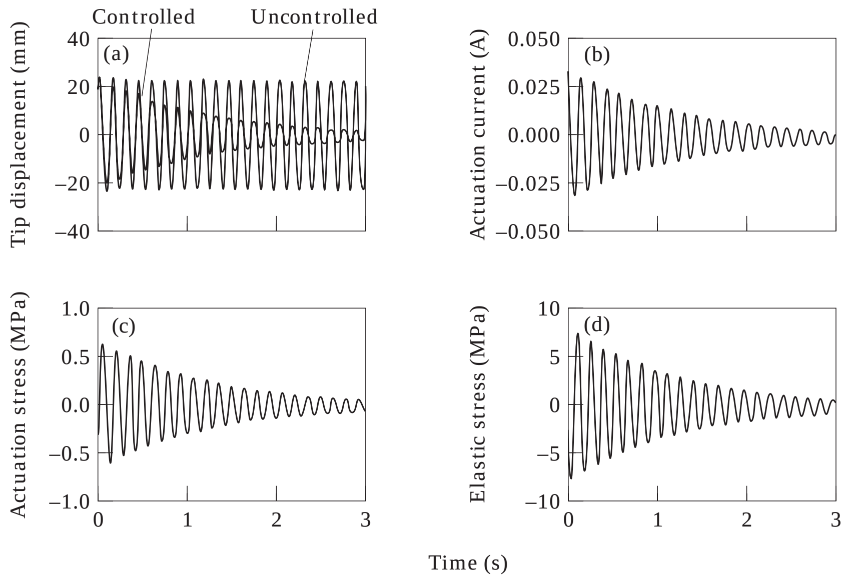

Figure 6. Vibration suppression: the fundamental of laminate 1 ($L_2 = 0{\cdot}1$ m, $L_3 = 0{\cdot}7$ m, $m_c = 31{\cdot}5$ kg/m, $m_0 = 1$ kg, $c = 10^5$, $n_0 = 10^5$ turns/m). (a) Variation of the tip displacement; (b) the control current in the tenth coil; (c) the actuation stress at $0{\cdot}095L$, (d) the elastic stress at $0{\cdot}095L$.

an initial velocity distribution along the span similar to each mode shape has been investigated adopting constant gain and a velocity proportional feedback control law. Detailed parametric study has been carried out to illustrate the effect of various parameters involved. The results indicate viability of developing cantilever beams with embedded magnetostrictive layers with a vibration suppression capability, for various applications such as robot manipulators and helicopter rotor blades.

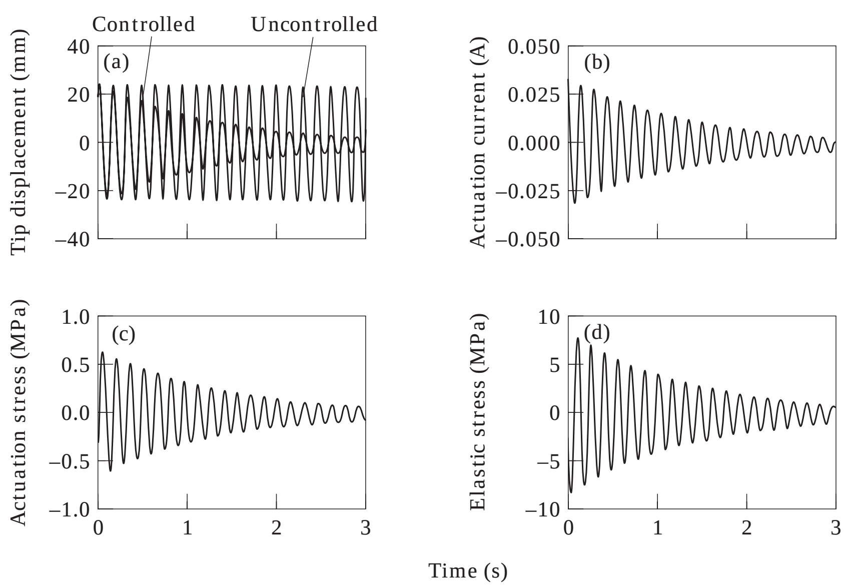

Figure 7. Vibration suppression: the fundamental of laminate 1 ($L_2 = 0{\cdot}1$ m, $L_3 = 0{\cdot}7$ m, $m_c = 31{\cdot}5$ kg/m, $m_0 = 3$ kg, $c = 10^5$, $n_0 = 10^5$ turns/m). (a) Variation of the tip displacement; (b) the control current in the tenth coil; (c) the actuation stress at $0{\cdot}095L$; (d) the elastic stress at $0{\cdot}095L$.

TABLE 6

The effect of control gain parameter c (laminate 1, $m_0 = 1$ kg, $L_3 = 0{\cdot}9L$)

Mode number	Case 1; $L_2 = 0{\cdot}2L$, $c = 10^4$, $n_0 = 10^4$ turns/m				Case 2; $L_2 = 0{\cdot}1L$, $c = 10^5$, $n_0 = 10^5$ turns/m			
	ω_d	α	t_s	I	ω_d	α	t_s	I
1	42·694	−0·261	15	0·8	42·689	−0·762	5	0·034
2	276·081	−4·167	1	0·4	275·412	−21·732	0·2	0·189
3	782·854	−7·866	0·5	0·8	776·208	−113·801	0·04	0·468
4	1531·531	−0·918	5	1·0	1513·353	−250·635	0·02	0·799

TABLE 7

Effect of flexural rigidity of the beam ($L_2 = 0{\cdot}1L$, $L_3 = 0{\cdot}7L$, $m_0 = 3$ kg, $m_c = 31{\cdot}5$ kg/m, $n_0 = 10^5$ turns/m, $c = 10^5$)

Mode number	$[90_9/\text{m}]$				$[0_9/\text{m}]$			
	ω_n	ω_d	α	ϕ	ω_n	ω_d	α	ϕ
1	20·919	20·908	−0·689	0·00013	62·023	62·019	−0·728	0·00006
2	137·769	136·379	−19·525	0·00129	409·164	408·601	−21·480	0·00043
3	359·061	349·125	−83·885	0·004671	1066·88	1062·675	−94·628	0·00136
4	739·722	712·785	−197·818	0·01023	2198·45	2186·299	−230·856	0·0028

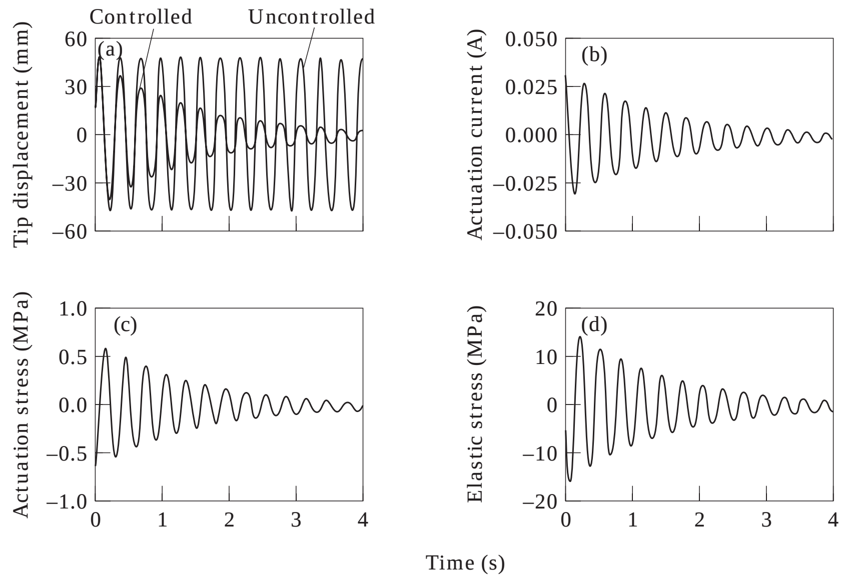

Figure 8. Vibration suppression: the fundamental of laminate $[90_9/\mathrm{m}]$ ($L_2 = 0{\cdot}1$ m, $L_3 = 0{\cdot}7$ m, $m_c = 31{\cdot}5$ kg/m, $m_0 = 3$ kg, $c = 10^5$, $n_0 = 10^5$ turns/m). (a) Variation of the tip displacement; (b) the control current in the tenth coil; (c) the actuation stress at $0{\cdot}095L$; (d) the elastic stress at $0{\cdot}095L$.

ACKNOWLEDGMENT

The research reported in this paper was partially supported by the Army Research Office under grant DAAL 03-92-G-0121, with Dr Gary Anderson as the Technical Monitor.

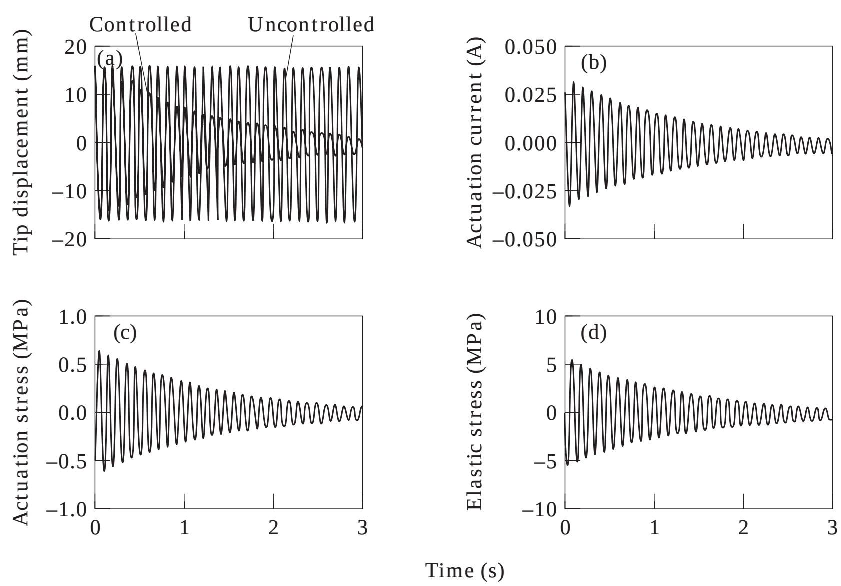

Figure 9. Vibration suppression: the fundamental of laminate $[0_9/\mathrm{m}]$ ($L_2 = 0{\cdot}1$ m, $L_3 = 0{\cdot}7$ m, $m_c = 31{\cdot}5$ kg/m, $m_0 = 3$ kg, $c = 10^5$, $n_0 = 10^5$ turns/m). (a) Variation of the tip displacement; (b) the control current in the tenth coil; (c) the actuation stress at $0{\cdot}095L$; (d) the elastic stress at $0{\cdot}095L$.

REFERENCES

1. T. Bailey and J. E. Hubbard, Jr. 1985 *Journal of Guidance*, *Control and Dynamics* **8**, 1199–1206. Distributed piezoelectric polymer active vibration control of a cantilever beam.
2. E. F. Crawley and J. De Luis 1987 *American Institute of Aeronautics and Astronautics Journal* **25**(10), 1373–1385. Use of piezoelectric actuators as elements of intelligent structures.
3. A. Baz, K. Imam and J. McCoy 1990 *Journal of Sound and Vibration* **140**, 437–456. Active vibration control of flexible beams using shape memory actuators.
4. E. M. Wise 1957 *Production Engineer*, 162–166 Magnetostriction: a new design tool.
5. R. S. Reed 1988 *Modelling and Simulation* **19**. Active vibration isolation using a magnetostrictive actuator.
6. M. W. Hiller, M. D. Bryant and J. Umegaki 1989 *Journal of Sound and Vibration* **134**, 507–519. Attenuation and transformation of vibration through active control of magnetostrictive Terfenol.
7. J. Dyberg 1986 1*st International Conference on Giant Magnetostrictive Alloys and Their Impact on Actuator and Sensor Technology*, *Marbella*, *Spain*. Magnetostrictive rods in mechanical applications.
8. R. G. Solomon, T. T. Hanson and F. K. Straub 1995 *Proceedings of SPIE—Smart Structures and Integrated Systems* (I. Chopra, editor), 28–37. Application of the magnetostrictive smart materials in rotor servoflap control.
9. M. Anjanappa and J. Bi 1994 *Smart Material and Structures*, **3**, 83–91. A theoretical and experimental study of magnetostrictive mini actuators.
10. M. Anjanappa and J. Bi 1994 *Smart Material and Structures* **3**, 383–390. Magnetostrictive mini actuators for smart structure application.
11. J. R. Vinson and R. L. Sierakowski 1990 *The Behavior of Structures Composed of Composite Material*. Dordrecht: Kluver Academic.
12. A. E. Clark 1980 *Ferromagnetic Materials*. Amsterdam: North-Holland. See Chapter 7: Magnetostrictive rare earth–Fe_2 compounds.
13. J. D. Kraus 1992 *Electromagnetics*, 233. New York: McGraw-Hill.

APPENDIX A: BOUNDARY VALUE PROBLEM

Substituting equations (2), (3) and (5) into equation (11), and then substituting equation (11) into (10) we obtain

$$A_{11}u_{,xx} - B_{11}v_{,xxx} - F_1 c\dot{v}_{,x} - m\ddot{u} = 0, \qquad -B_{11}u_{,xxx} + D_{11}v_{,xxxx} + F_2 c\dot{v}_{,xx} + m\ddot{v} = 0, \quad \text{(A1)}$$

where

$$A_{11}, B_{11}, D_{11} = \sum_{i=1}^{n} \int_{y_i}^{y_{i+1}} \bar{Q}_{11}^{(i)}(1, y, y^2)\,\mathrm{d}y,$$

$$F_{11}, F_{22} = \int_{y_m}^{y_{m+1}} E_m\,\mathrm{d}(1, y)\,\mathrm{d}y, \qquad m = \sum_{i=1}^{n} \int_{y_i}^{y_{i+1}} \rho^{(i)}\,\mathrm{d}y. \quad \text{(A2)}$$

The boundary conditions at $x = 0$ and L are,

$$\text{either} \quad v = 0 \quad \text{or} \quad B_{11}u_{,xx} - D_{11}v_{,xxx} - F_2 c\dot{v}_{,x} = 0,$$

$$\text{either} \quad v_{,x} = 0 \quad \text{or} \quad B_{11}u_{,x} - D_{11}v_{,xx} - F_2 c\dot{v} = 0,$$

$$\text{either} \quad u = 0 \quad \text{or} \quad A_{11}u_{,x} - B_{11}v_{,xx} - F_2 c\dot{v} = 0. \quad \text{(A3)}$$

The above formulation is valid for the entire length of the beam since the lay-up is uniform. The existence of actuation stresses in the region $0 \leqslant x \leqslant L_2$ will enter the Galerkin technique through the integral and causes no serious formulation errors.

Broadly, there are two alternative ways to obtain the solution. The first method consists of obtaining a direct solution to the governing differential equations. Following the second method, the solution is obtained in a Galerkin sense by starting with a suitable admissible function and using equation (10). The second approach is adopted in this paper.

APPENDIX B: NOMENCLATURE

A, B, D, M_1, M_2	cross-sectional constants
c	control gain parameter
d	magnetomechanical coupling coefficient
$E_{11}, E_{22}, G_{12}, v_{12}$	material constants of CFRP layer
E_m	Young's modulus of the magnetostrictive layer
F_1, F_2	control force parameters
g	control gain
H	magnetic field intensity
$I(x, t)$	coil current
i	number of layer
k_1	coil constant
L	span of the beam
L_1, L_2	starting and end position of coils on the span
L_3	location of the concentrated mass
l	length of the coil
m_0	concentrated mass
m	mass of the beam per unit length of span
m_c	mass of the coil per unit length of span
N	number of turns in the coil
n_c	number of turns in the coil
n_0	number of turns per unit length
Q_{ij}	reduced elastic constant of CFRP layers
$\bar{Q}_{ij}$	transformed reduced elastic constant of CFRP layers
r_c	coil radius
S	compliance of the magnetostrictive layer
T_e	kinetic energy of the beam
t_1, t_2	time instant
U, V, W	displacement along x, y, z-axes respectively
U_e	strain energy of the beam
u, v	displacement along x- and y-axis
w_c	width of the coil
x, y, z	Cartesian coordinates
Y_1, Y_2	amplitude of the generalized time coordinate
α	exponent representative of vibration suppression
δ	variational symbol
ε	strain
θ	orientation of fibers with respect to x-axis
Λ_1, Λ_2	generalized time coordinate
λ	eigenvalue
v	Poisson ratio
ρ	mass density of CFRP layers
ρ_m	mass density of magnetostrictive layer
σ	stress
σ_a	actuation stress
ϕ	amplitude ratio of longitudinal displacement to transverse displacement
Ω	total volume of the beam
ω_n	natural frequency of the beam without control
ω_d	frequency of the beam with control
$\langle \dot{} \rangle$	time derivative of $\langle\ \rangle$
$\langle\ \rangle_{,x}$	derivative of $\langle\ \rangle$ with respect to x